Electron-hole superfluidity controlled by a periodic potential

Oleg L. Berman, Roman Ya. Kezerashvili, Yurii E. Lozovik, Klaus G. Ziegler

Angaben zur Veröffentlichung / Publication details:

Berman, Oleg L., Roman Ya. Kezerashvili, Yurii E. Lozovik, and Klaus G. Ziegler. 2019. "Electron-hole superfluidity controlled by a periodic potential." *Physical Review B* 100 (13): 134514. https://doi.org/10.1103/physrevb.100.134514.

Electron-hole superfluidity controlled by a periodic potential

Oleg L. Berman,[1,2] Roman Ya. Kezerashvili,[1,2] Yurii E. Lozovik,[3,4] and Klaus G. Ziegler[5]

[1]*Physics Department, New York City College of Technology, The City University of New York, Brooklyn, New York 11201, USA*

[2]*The Graduate School and University Center, The City University of New York, New York, New York 10016, USA*

[3]*Institute of Spectroscopy, Russian Academy of Sciences, 142190 Troitsk, Moscow, Russia*

[4]*Research University Higher School of Economics, 101000 Moscow, Russia*

[5]*Institut für Physik, Universität Augsburg, D-86135 Augsburg, Germany*

(Received 22 June 2019; revised manuscript received 7 October 2019; published 28 October 2019)

We propose controlling an electron-hole superfluid in semiconductor coupled quantum wells and double layers of a two-dimensional (2D) material by an external periodic field. This can be created either by the gates periodically located and attached to the quantum wells or double layers of the 2D material or by the moiré pattern of two twisted layers. The dependence of the electron-hole pairing order parameter on the temperature, the charge carrier density, and the gate parameters is obtained by minimization of the mean-field free energy. The second-order phase transition between superfluid and electron-hole plasma, controlled by the external periodic gate field, is analyzed for different parameters.

DOI: 10.1103/PhysRevB.100.134514

I. INTRODUCTION

The system of spatially separated electrons and holes can be realized in semiconductor coupled quantum wells (CQWs), where electrons and holes are located in different quantum wells. For low temperatures and weak attraction the BCS approach describes the superfluid formed by coherent Cooper pairs, while in the strong-attraction regime the composite bosons, known as indirect (dipolar) excitons, are formed. An electron-hole plasma (EHP) appears at sufficiently high temperatures. Superfluidity in the two-dimensional (2D) system with spatially separated electrons and holes was predicted using the BCS mean-field approach [1], which caused intensive theoretical [2–11] as well as experimental studies [12–23]. Different electron-hole phases, characterized by unique collective properties, have been analyzed in the system of spatially separated electrons and holes [24]. The BCS phase of electron-hole Cooper pairs in a dense electron-hole system [1] and a dilute gas of indirect excitons, which formed as bound states of electron-hole pairs, were also analyzed in CQWs [25]. Superfluidity of the BCS phase, formed by spatially separated electrons and holes, can be manifested as nondissipative electric currents and quasi-Josephson phenomena [1,2]. Besides the superfluid phase a Wigner supersolid state caused by dipolar repulsion in electron-hole double layers was described [26–29]. Recent theoretical and experimental achievements in the studies of the superfluid dipolar exciton phases in CQWs were reviewed in Ref. [30]. Probing the ground state of an electron-hole double layer by low-temperature transport was experimentally performed [31], and the various experimental studies of excitonic phases in CQWs were described in Ref. [32].

Another physical realization of indirect excitons, formed in an electron-hole double layer, is a wide single GaAs/AlGaAs quantum well with a finite width [33]. In a wide single QW, the transverse electric field separates electrons and holes at the different boundaries of the QW [33]. The advantage of a wide single QW compared with CQWs is the smaller number of QW boundaries, which leads to the increase of the electron mobility. Based on the photoluminescence pattern caused by electron-hole recombination, evidence of a condensate of indirect excitons, electrically polarized in a GaAs wide single QW, was found experimentally recently for a 15-nm-thick quantum well at temperature $T = 370$ mK [34]. A spontaneous condensation of trapped two-dimensional dipolar excitons from an interacting gas into a dense liquid state was observed in GaAs/AlGaAs CQWs with an interwell separation $D = 4$ nm at temperatures below a critical temperature $T_c \approx 4.8$ K [35]. The transport of indirect excitons with an interwell separation $D = 4$ nm in GaAs/AlGaAs CQWs in linear lattices, created by laterally modulated gate voltage with a lattice period $b = 2$ μm, was studied experimentally at the temperatures $T = 1.6$ K and $T = 6$ K, and the localization-delocalization transition for transport across the lattice was observed by reducing the lattice amplitude or increasing the exciton density [36].

Besides semiconductor CQWs, the superfluid system of spatially separated electrons and holes can appear in a graphene double layer [11,37–40], two opposite surfaces of the film of topological insulators [41], and two layers with composite fermions in the quantum Hall regime at filling factor $\nu = 1/2$ [42]. Such systems can be engineered with a WSe_2 barrier between the graphene layers to enhance the interlayer tunneling [23].

Today, an intriguing counterpart to gapless graphene is a class of monolayer direct band gap materials, namely, transition-metal dichalcogenides (TMDCs). Monolayers of TMDCs such as MoS_2, $MoSe_2$, $MoTe_2$, WS_2, WSe_2, and WTe_2 are 2D semiconductors, which have a variety of applications in electronics and optoelectronics [43]. The strong

interest in TMDC monolayers is motivated by the following facts: a semiconductor band structure is characterized by a direct gap in the single-particle spectrum [44], the existence of excitonic valley physics, and the possibility of electrically tunable, strong light-matter interactions [45,46]. Monolayers of transition-metal dichalcogenides are truly 2D semiconductors, which hold great appeal for electronics and optoelectronics applications due to their direct band gap properties. Monolayer TMDCs have already been implemented in field-effect transistors, logical devices, and lateral and tunneling optoelectronic structures [43]. Like graphene, the monolayer TMDCs have hexagonal lattice structures, and the nodes (valleys) in the dispersion relations of both the valence and conduction bands can be found at the $\mathbf{K}$ and $-\mathbf{K}$ points of the hexagonal Brillouin zone. However, unlike graphene, these 2D crystals do not have inversion symmetry [43].

High-temperature superfluidity can be studied in a heterostructure of two TMDC monolayers, separated by a hexagonal boron nitride (h-BN) insulating barrier [47]. The dipolar excitons were observed in heterostructures formed by monolayers of MoS_2 on a substrate constrained by hexagonal boron nitride layers [48]. The theoretical study of the phase diagram of 2D condensates of indirect excitons in a TMDC double layer was reported [49]. The high-temperature superfluidity of the two-component Bose gas of A and B dipolar excitons in a transition-metal dichalcogenide double layer was predicted in Refs. [50,51].

In this paper we study how the BCS-like EHP-superfluid phase transition can be controlled by the external periodic field, applied to the spatially separated electrons and holes via the gates periodically attached to CQWs, where a quasi-two-dimensional system of charge carriers is formed. The external periodic field, applied to the spatially separated electrons and holes, can also be produced via the gates periodically attached to double layers of a 2D material or a twisted TMDC double layer, where a truly 2D system of charge carriers is formed. For this purpose we employ a mean-field approximation for the many-body system of electrons and holes, using the partition function of the grand-canonical ensemble at temperature T and the chemical potentials of the electrons and the holes, respectively. The latter represent the Fermi energies of the electrons and the holes. The logarithm of the partition function gives us immediately the free energy, whose minimum defines the mean-field solution with a nonvanishing order parameter of the superfluid phase. The main goal is to analyze the influence of the external periodic field on the critical temperature of the EHP-superfluid transition in an electron-hole double layer. Here it should be mentioned that the phase fluctuations of the order parameter can lead to a vortex-pair dissociation, which results in a nonsuperfluid Kosterlitz-Thouless phase. Its critical temperature is close to the mean-field temperature if the exciton-exciton interaction is weak [52].

This paper is organized in the following way. We obtain the free energy of the electron-hole double layer in the external periodic potential and study the second-order EHP-superfluid transition using a Landau expansion of the free energy in Sec. II. The results of the calculations are presented and analyzed in Sec. III. Finally, a discussion of the results and the conclusions follow in Sec. IV.

II. PHASE TRANSITION IN THE ELECTRON-HOLE DOUBLE LAYER UNDER THE ACTION OF THE EXTERNAL PERIODIC POTENTIAL

The Hamiltonian of a system of spatially separated electrons and holes in the momentum representation can be written as

$$H=\sum_{\mathbf{p}}\sum_{\sigma=e,h}\varepsilon_{\mathbf{p},\sigma}c^{\dagger}_{\mathbf{p}\sigma}c_{\mathbf{p}\sigma}+\sum_{\mathbf{p},\mathbf{p}_1,\mathbf{p}_2}U_{\mathbf{p}}c^{\dagger}_{\mathbf{p}-\mathbf{p}_1,h}c_{\mathbf{p}-\mathbf{p}_2,h}c^{\dagger}_{\mathbf{p}_1,e}c_{\mathbf{p}_2,e}, \tag{1}$$

where $c^{\dagger}_{p,e}$ ($c_{p,e}$) is the creation (annihilation) operator for electrons and $c^{\dagger}_{p,h}$ ($c_{p,h}$) is the corresponding operator for holes. The electron and hole single-particle dispersion $\varepsilon_{\mathbf{p},\sigma}$ depends on the details of the material properties. Moreover, it is sensitive to an additional periodic potential, applied to the CQWs or double layers of the 2D material. An example is a periodic potential in the form of a square lattice with periodicity b. Then the electron and hole dispersion reads [53–55]

$$\varepsilon_{\mathbf{p}}=\delta_0-2t\cos(p_xb/\hbar)-2t\cos(p_yb/\hbar)\ (-\pi\leqslant p_{x,y}b/\hbar<\pi), \tag{2}$$

which has a band width $8t$ and a Fermi energy δ_0. The electron-hole attraction potential in momentum space $U_{\mathbf{p}}$ is discussed briefly below. In Eq. (1) the spins of electrons and holes are neglected because we are not interested in magnetization effects.

We consider an external periodic potential induced by the gate forming either a one-dimensional (1D) or a 2D square superlattice with a period b applied to the electron and hole quantum wells. An example is the particular case related to the phase transition of indirect excitons in a double layer, formed by two TMDC monolayers that are separated by h-BN since h-BN monolayers are characterized by a relatively small density of the defects of their crystal structure monolayers. In Fig. 1 a schematic electrode pattern in the x-y and z-x planes is presented. In our calculations we consider the TMDC monolayers to be separated by h-BN insulating layers and the separation between two layers of TMDC materials calculated in steps of $D_{\mathrm{hBN}}=0.333$ nm, corresponding to the thickness of one h-BN monolayer [47]. Therefore, the interlayer separation D is presented as $D=N_LD_{\mathrm{hBN}}$, where N_L is the number of h-BN monolayers, placed between two TMDC monolayers. It is obvious that the strength of the electron-hole interaction decreases with the increase of the separation between the layers. We assume that the densities of electrons and holes are equal in order to have a neutral electron-hole plasma and because the electrons and holes are created always pairwise by an external laser source. This implies that the corresponding chemical potentials are also equal. Periodically positioned gates under the same electric potentials create in turn the periodical potential in the 2D system under consideration.

When the electron-hole attraction leads to Cooper pairing of electrons and holes, characterized by the order parameter Δ [56,57], the free energy is described within the mean-field approximation (MFA) [1,58]. Following Ref. [58] and assuming that (i) the order parameter Δ does not depend on the

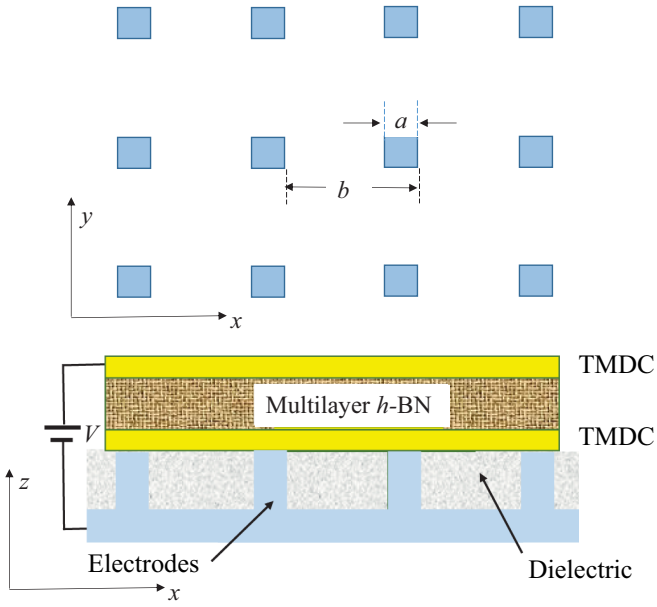

FIG. 1. Schematic electrode pattern in the x-y and z-x planes.

momentum and (ii) the dispersion relation $\varepsilon_{\mathbf{p},e} = \varepsilon_{\mathbf{p},h} = \varepsilon_{\mathbf{p}}$ is the same for electrons and holes, the MFA of the free energy at temperature T ($\beta = 1/k_B T$, where k_B is the Boltzmann constant) as a function of the dimensionless order parameter $\gamma = \beta|\Delta|$ can be written as

$$F = -\frac{1}{\beta^2 u_0}\gamma^2 - \frac{1}{|B|\beta}\int_B \ln\left\{2\left[1+\cosh\left(\sqrt{\beta^2\varepsilon_{\mathbf{p}}^2+\gamma^2}\right)\right]\right\}d^2p. \quad (3)$$

In Eq. (2) the integration over the momentum $\mathbf{p}$ is taken over the Brillouin zone with area $|B|$, and u_0 is the strength of the electron-hole interaction given by

$$\frac{1}{u_0} = \frac{1}{|B|}\int_B \frac{1}{U_{\mathbf{p}}}d^2p < 0, \quad (4)$$

which parametrically depends on the interlayer separation D. The effective electron-hole potential $U_{\mathbf{p}}$ and therefore the electron-hole pairing parameter u_0 in the general case depend essentially on the screening of the Coulomb potential. This issue, in particular the different effects of static screening and dynamical screening in a many-electron and -hole system, has been discussed intensively in the literature [59–65]. In particular, in two-dimensional semiconductors (contrary to the three-dimensional case) the dielectric function is nonlocal; that is, it depends on the wave vector [66]. This leads to the Ritova-Keldysh potential between two charges [67,68]. The Ritova-Keldysh potential has been widely used to describe the Coulomb interaction of few-body complexes in a monolayer of TMDCs and beyond (see the review in [69] and references therein).

The mean-field free energy (3) indicates that the lattice structure and the additional periodic potential enter our calculation only through the dispersion $\varepsilon_{\mathbf{p}}$. In Eq. (5) we will see that the condition for the critical temperature of the transition to a superfluid state at a given electron-hole coupling parameter u_0 depends only on the density of states of particles with dispersion $\varepsilon_{\mathbf{p}}$ and on the Fermi energy δ_0.

We can rewrite Eq. (2) in the form of a dimensionless free energy $f = -u_0 F/(k_B T)^2$ and expand the latter in terms of the order parameter γ^2 as $f = f_0 + f_2\gamma^2 + f_4\gamma^4$ (Landau expansion [70,71]). The corresponding coefficients for this expansion are given in Appendix A by Eqs. (A4)–(A6). At the point of the phase transition we have a zero order parameter $\gamma = 0$, and the condition for the minimum of the free energy is $\frac{\partial f}{\partial \gamma^2}|_{\gamma=0} = f_2 = 0$. Therefore, the critical point is defined by a vanishing coefficient f_2. Thus, from expression (A5) it follows that the critical inverse temperature β_c satisfies the condition

$$\frac{1}{u_0} = -\frac{1}{|B|}\int_B \frac{\tanh(\beta_c|\epsilon_{\mathbf{p}}|)}{|\epsilon_{\mathbf{p}}|}d^2p = -\int_{E_0}^{E_1}\frac{\tanh(\beta_c|2tE-\delta_0|)}{|2tE-\delta_0|}\rho(E)dE. \quad (5)$$

Here we have used the fact that the p integration can be expressed as an energy integration through the relation $d^2p/|B| = \rho(E)dE$, where $\rho(E)$ is the density of states of the noninteracting Hamiltonian with dispersion $\varepsilon_{\mathbf{p}}$. The dimensionless energy parameter $E = (\delta_0 - \varepsilon_{\mathbf{p}})/2t$ is derived from the dispersion which is shifted by the Fermi energy δ_0. The integration is restricted to the interval $[E_0, E_1]$ since only electronic states are accessible within the main band of the electronic band structure. The specific values depend on the material and its dispersion; typically, for a parabolic dispersion they are given by $E_0 \approx 0$ and $E_1 \approx \hbar^2/(\lambda^2 2m)$ with the lattice constant λ of the underlying material. According to Eq. (5), the temperature of the electron-hole pairing is controlled by the electron-hole pairing parameter (i.e., by the effective electron-hole potential), by the density of states, which is essentially modified by the external periodic potential, and by the position of the Fermi energy. The relation between u_0 and β_c in Eq. (5) indicates that an increasing interaction strength $-u_0$ implies an increasing critical temperature. Moreover, $\tanh(\beta_c|2tE-\delta_0|)/|2tE-\delta_0|$ is a monotonically decreasing function of $|2tE-\delta_0|$ with the maximum at $E = \delta_0/2t$. The density of states $\rho(E)$, on the other hand, distinguishes between the case of a parabolic dispersion [$\rho(E) = \text{const}$] and the case of a periodic potential, where $\rho(E)$ is not constant. Thus, the goal is to design the dispersion by adding a superstructure to the material. This can be achieved by doping [72], by creating a gated periodic potential on the 2D material [36] (see Fig. 1), or by twisting the two layers relative to each other to create a moiré pattern [73,74]. A particular possibility to tune to a higher critical temperature is to create Van Hove singularities near the Fermi level of two twisted graphene bilayers [75–78]. The Van Hove singularities, which appear at the saddle points on the Brillouin zone, can also be shifted towards the Fermi energy by applying strain to graphenelike materials [79]. In terms of an additional periodic potential, the effect of strain can be simulated by an anisotropic potential. Then the density of states can be chosen such that it picks up the maximum value of the integrand $\tanh(\beta_c|2tE-\delta_0|)/|2tE-\delta_0|$. Although this depends on the Fermi energy δ_0, the latter can also be tuned by a uniform external gate to obtain a large value for the

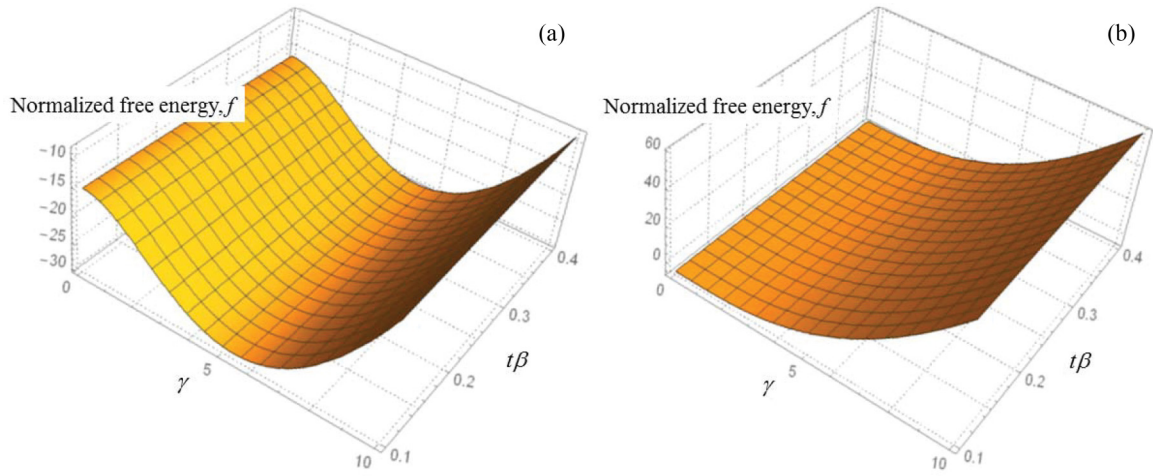

FIG. 2. The normalized free energy f as a function of $t\beta$ and the order parameter γ. (a) $\delta_0/2t = 0.15$, $\beta u_0 = -80$. (b) $\delta_0/2t = 0.15$, $\beta u_0 = -30$.

integral. The idealized case would be $\rho(E) = \delta(E - \delta_0/2t)$, which provides the maximal critical temperature

$$k_B T_c = -u_0. \tag{6}$$

If $\rho(E) = \delta(E - E')$, where E' is a characteristic parameter of the model, we get from Eq. (5)

$$k_B T_c = -u_0 \frac{|2tE' - \delta_0|/u_0}{\operatorname{arctanh}(|2tE' - \delta_0|/u_0)}. \tag{7}$$

As an example we consider the tight-binding approximation of Eq. (2). The corresponding density of states reads [80]

$$\rho(E) = \rho_0 \frac{K\left(\frac{2-|E|}{2+|E|}\right)}{2+|E|} \quad (-2 \leqslant E \leqslant 2), \tag{8}$$

where $K(x)$ is the complete elliptic integral of the first kind and ρ_0 is a normalization factor. Appendix B gives the expressions for coefficients f_0, f_2, and f_4 of the Landau expansion in the case of the periodical potential. For the dispersion (2) we have derived some results directly from Eqs. (3) and (5), which will be discussed in the next section.

Instead of the 2D periodic potential we could also consider an anisotropic potential with a 1D periodicity, which would also strongly affect the density of states. This case corresponds to the system studied in Ref. [36] and was previously considered for stripes in superconductors [81,82] and in coupled graphene nanoribbons [83], where the goal is to create Van Hove singularities in the density of states. A one-dimensional periodic potential has an inverse square-root singularity at $E = 0$, which can result in an even stronger enhancement of the critical temperature. In that case we must use the density of states $\rho(E_x)$ for a potential varying in the x direction. Then the condition in Eq. (5) becomes

$$\frac{1}{u_0} = -\frac{1}{p_1 - p_0} \int_{p_0}^{p_1} \int_{E_0}^{E_1} \frac{\tanh\left(\beta_c \left|2tE_x + p_y^2/2m - \delta_0\right|\right)}{\left|2tE_x + p_y^2/2m - \delta_0\right|} \times \rho(E_x) dE_x dp_y, \tag{9}$$

where p_0 and p_1 are the band edges in the y direction and E_0 and E_1 are the band edges in the x direction of the considered model.

III. RESULTS

The free energy F of Eq. (3) with the dispersion in Eq. (2) is calculated as a function of the dimensionless order parameter γ. The dependence of the dimensionless free energy $f = -\beta^2 u_0 F$ on $t\beta$ and the order parameter γ is shown in Fig. 2. This result demonstrates that f has a minimum with respect to the order parameter γ, while the dependence of f on $t\beta$ is not strong. The nonzero minimum of f with respect to the order parameter γ corresponds to the equilibrium value of γ, characterizing the electron-hole superfluid. The plot in Fig. 2(a) represents the low-temperature BCS-like superfluid for electron-hole pairing with a nonzero value of the order parameter $\gamma > 0$ at the minimum, while Fig. 2(b) shows the high-temperature nonsuperfluid EHP for the zero value of γ at the minimum. Both cases are connected via the second-order phase transition, as visualized in Fig. 3, where the normalized free energy f as a function of the order parameter

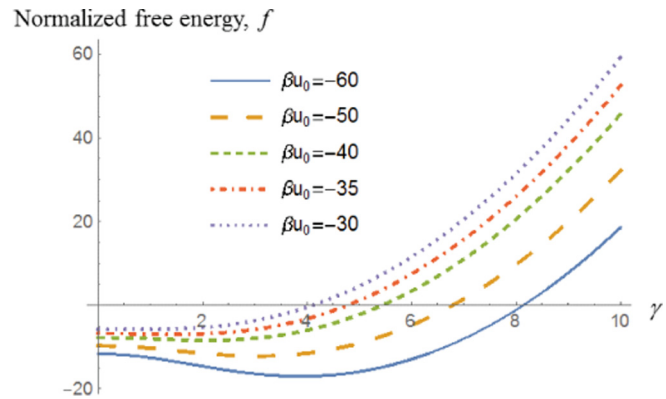

FIG. 3. The normalized free energy f for $\beta u_0 = -30, -35, -40, -50, -60$ at $\beta t = 0.22$ and $\delta_0/2t = 0.175$ indicates a second-order phase transition between $\beta u_0 = -50$ and $\beta u_0 = -40$.

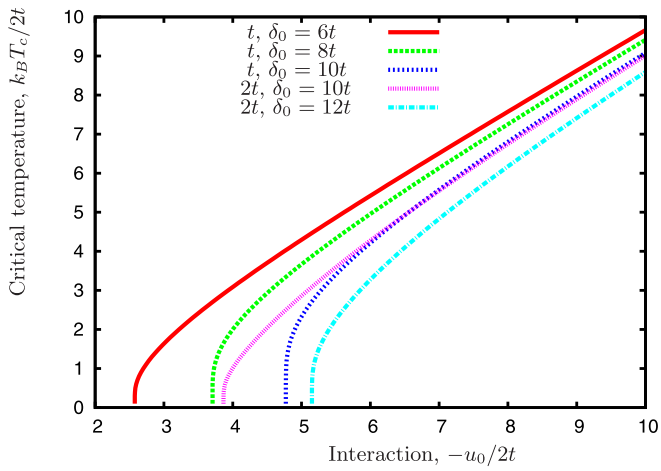

FIG. 4. Critical temperature as a function of the interaction parameter for the square lattice potential with different Fermi energies δ_0 and with potential strength t or $2t$ in Eq. (2).

γ is plotted for different values of βu_0 at fixed parameters $t\beta$ and $\delta_0/2t$. The curves for $\beta u_0 = -50$ and $\beta u_0 = -60$ demonstrate the existence of a low-temperature BCS-like superfluid with electron-hole pairing with a nonzero equilibrium value of the order parameter $\gamma > 0$. The second-order phase transition is characterized by the equilibrium value $\gamma = 0$, which corresponds to the values of the parameter βu_0 between $\beta u_0 = -50$ and $\beta u_0 = -40$, as shown in Fig. 3. According to Fig. 3, for fixed parameters $\delta_0/2t$ and $t\beta$, the minimal order parameter γ increases with decreasing βu_0 if $\beta u_0 < -50$. The curves in Fig. 3 for $\beta u_0 = -30$ and $\beta u_0 = -35$ represent the high-temperature nonsuperfluid EHP with $\gamma = 0$. Figure 4 can be understood as a k_BT-u_0 phase diagram, in which the different curves indicate the phase boundaries between the EHP on the left and the superfluid on the right for different values of the Fermi energy in the case of a periodic potential with dispersion (2). The critical temperature depends on the interaction strength u_0, the chemical potential δ_0, and the strength of the periodic potential t. For a given u_0 and a given potential strength t the critical temperature k_BT_c can be found in units of $2t$ for different values of δ_0. The critical interaction strength, where the graphs start at $T_c = 0$, increases with increasing δ_0. Obviously, we need $-u_0 > 4t$ to obtain a superfluid phase of excitons if $\delta_0 > 6t$. Since the dispersion must be positive [i.e., $\varepsilon_{\mathbf{p}} > 0$ in Eq. (2)], we have $\delta_0 > 4t$. On the other hand, the critical temperature increases with t, as we can see in Fig. 4 when we double the strength of the periodic potential by $t \to 2t$ at fixed $\delta_0 = 10t$. For a large interaction strength the critical temperature indicates a linear behavior, which is below the ideal relation of Eq. (6), however. As a typical example, we assume $u_0 = -8$ meV and $t = 1$ meV such that $-u_0/2t = 4$. Together with Fig. 4 we get $T_c = 40$ K for $\delta_0 = 10$ meV and $T_c = 120$ K for $\delta_0 = 6$ meV. Assuming that u_0 and t can be independently chosen, where u_0 is a property of the layer material and t depends on the applied electric gates, is an oversimplification. In a more realistic consideration these two parameters depend on each other due to the geometry of the gates and the distance between layers. This can be calculated in a classical capacitor model, as briefly discussed in Appendix C.

IV. DISCUSSION AND CONCLUSIONS

In the framework of the mean-field approach for electron-hole pairing, we applied the tight-binding approximation for the single-electron spectrum of the superlattice created by the external periodic potential and studied the effect of an additional periodic potential on the EHP-superfluid transition. We have assumed for simplicity that the dispersion and the Fermi surfaces of the electrons and the holes are the same and analyzed the phase transition at finite temperatures. Our results clearly indicate the possibility to control the electron-hole superfluid in CQWs or double layers of a 2D material by applying an external periodic potential due to an attached periodic gate. An alternative approach is to create a tunable periodic lattice in two twisted layers of 2D materials ("magic angle" bilayers) [84]. The analogous effect occurs in a supersolid, where the crystalline long-range order and noncrystalline long-range order coexist [85–87]. In contrast to a supersolid, where the crystalline phase is formed due to self-organization, the band structure in the system under consideration is induced by the external periodic potential.

A periodic potential creates many bands which are typically separated by gaps. (Neighboring bands can also touch each other at spectral nodes. This case, however, is not considered here.) To reduce the calculation to a single band we have assumed that the order parameter $|\Delta|$ is smaller than the gap between the neighboring band. This allows us to use a single band projection, based on a tight-binding model. The single band has a lower band edge at energy E_0 and an upper band edge at energy E_1, which are the boundaries of integration for the condition of the critical temperature in Eq. (5). The $\mathbf{k}$ integration is determined by the Coulomb interaction. In the BCS theory of Cooper pairs only a small interval around the Fermi energy, whose width is given by the Debye energy $\hbar\omega_D$, contributes to an attractive interaction: $E_0 = E_F - \hbar\omega_D$, $E_1 = E_F + \hbar\omega_D$ [56,88]. This is different in the excitonic case because the attractive Coulomb interaction exists for all energies inside the band.

The critical temperature depends on the interaction strength u_0, the chemical potential δ_0, and the strength of the periodic potential t. This is visualized in Fig. 4, where for a given u_0 and a given potential strength t the critical temperature k_BT_c can be found in units of $2t$ for different values of δ_0.

A critical assumption in our model is that electrons and holes have the same dispersion. If they had different dispersions, we would expect a more complex phase diagram (cf. Ref. [58]). A difference in the dispersions can even affect the form of the order parameter. In our study we assume that the pumping beam is circularly polarized, and hence, the excitons are formed only in one of the valleys: $\mathbf{K}$ or $-\mathbf{K}$ [45,46]. In this study we address the formation of excitons in one of the valleys. Moreover, we can have two electronic species in TMDC materials due to the existence of two valleys [89].

It should be of particular interest to extend our MFA approach to a more complex one with the valley degrees of freedom and the effective coupling between the two valleys

included. Another interesting extension of the MFA of the present work would be the inclusion of quantum fluctuations. This would open a wide avenue for measurements of quantum effects near the EHP-superfluid transition as well as inside the EHP and the superfluid through quantum excitations. A first step in this direction was the calculation of the density-density correlation and the structure factor, which indicates a characteristic increase near the transition [90]. Another possibility is to determine quantum transport properties in the EHP and the superfluid.

ACKNOWLEDGMENTS

O.L.B. and R.Ya.K. were supported by the U.S. Department of Defense under Grant No. W911NF1810433. Yu.E.L. was supported by the Program of Basic Research of HSE and RFBR Grants No. 17-02-01134 and No. 18-52-00002. K.G.Z. is grateful for support through a grant from the Julian Schwinger Foundation.

APPENDIX A: EXPANSION OF FREE ENERGY WITH RESPECT TO THE ORDER PARAMETER IN LANDAU FORM

From Eq. (3) the dimensionless free energy $f = -u_0 F/(k_B T)^2$ can be written as

$$f = \gamma^2 + u_0\beta\frac{1}{|B|}\int_B \ln\left\{2\left[1+\cosh\left(\sqrt{\beta^2\varepsilon_{\mathbf{p}}^2+\gamma^2}\right)\right]\right\}d^2p. \tag{A1}$$

One can expand the integrant in Eq. (A1) in terms of the power of γ^2 as

$$\begin{aligned}&\ln\left\{2\left[1+\cosh\left(\sqrt{\beta^2\varepsilon_{\mathbf{p}}^2+\gamma^2}\right)\right]\right\}\\ &\quad= \ln[2(1+\cosh[\beta|\varepsilon_{\mathbf{p}}|)] + \frac{\tanh\left(\frac{1}{2}\beta|\varepsilon_{\mathbf{p}}|\right)}{2\beta|\varepsilon_{\mathbf{p}}|}\gamma^2\\ &\qquad+\frac{\beta^2\varepsilon_{\mathbf{p}}^2-\beta|\varepsilon_{\mathbf{p}}|\sinh(\beta|\varepsilon_{\mathbf{p}}|)}{8\beta^4\varepsilon_{\mathbf{p}}^4(1+\cosh[\beta|\varepsilon_{\mathbf{p}}|])}\gamma^4+\cdots.\end{aligned} \tag{A2}$$

Here to obtain the final expression for the coefficients of the expansion we have used the following identities:

$$\sinh 2u = 2\sinh u\cosh u, \quad 1+\cosh 2u = 2\cosh^2 u. \tag{A3}$$

Substituting (A2) into Eq. (A1), we present the dimensionless free energy in the Landau form [70,71],

$$f = f_0 + f_2\gamma^2 + f_4\gamma^4 + \cdots,$$

where

$$f_0 = u_0\beta\frac{1}{|B|}\int_B \ln\{2[1+\cosh(\beta|\varepsilon_{\mathbf{p}}|)]\}d^2p, \tag{A4}$$

$$f_2 = 1 + u_0\beta\frac{1}{|B|}\int_B \frac{\tanh\left(\frac{1}{2}\beta|\varepsilon_{\mathbf{p}}|\right)}{2\beta|\varepsilon_{\mathbf{p}}|}d^2p, \tag{A5}$$

$$f_4 = u_0\beta\frac{1}{|B|}\int_B \frac{\beta^2\varepsilon_{\mathbf{p}}^2-\beta|\varepsilon_{\mathbf{p}}|\sinh(\beta|\varepsilon_{\mathbf{p}}|)}{8\beta^4\varepsilon_{\mathbf{p}}^4(1+\cosh[\beta|\varepsilon_{\mathbf{p}}|])}d^2p. \tag{A6}$$

APPENDIX B: FREE ENERGY IN THE CASE OF THE PERIODIC POTENTIAL

In the case of the periodic potential, the integration in (A1) as well as in Eqs. (A4)–(A6) is taken over the Brillouin zone, implying $|B|$ is the area of the Brillouin zone (for the square superlattice of the period b): $|B| = (2\pi\hbar)^2/b^2$; therefore, the limits of the integration over p_x and p_y are given by $-\pi\hbar/b$ and $-\pi\hbar/b$. Assuming that in (A4)–(A6) the single-particle energy dispersions versus momentum for electrons and holes are the same, we can calculate f_0, f_2, and f_4:

$$f_0 = u_0\beta\int_{-2}^{2}\frac{\ln\{2[1+\cosh(\beta|\delta_0-2tE|)]\}K\left(\frac{2-|E|}{2+|E|}\right)}{2+|E|}dE, \tag{B1}$$

$$f_2 = 1 + u_0\beta\int_{-2}^{2}\frac{\tanh\left(\frac{1}{2}\beta|\delta_0-2tE|\right)K\left(\frac{2-|E|}{2+|E|}\right)}{2|\delta_0-2tE|(2+|E|)}dE, \tag{B2}$$

$$\begin{aligned}f_4 = u_0\beta\int_{-2}^{2}&\frac{\beta^2(\delta_0-2tE)^2-\beta|\delta_0-2tE|\sinh(\beta|\varepsilon_{\mathbf{p}}|)}{8\beta^4(\delta_0-2tE)^4\{1+\cosh[\beta|(\delta_0-2tE|)]\}}\\ &\times\frac{K\left(\frac{2-|E|}{2+|E|}\right)}{(2+|E|)}dE,\end{aligned} \tag{B3}$$

where $K(k)$ is the complete elliptic integral of the first kind.

APPENDIX C: EFFECTIVE INTERACTION STRENGTH u_0

We consider a classical approximation of a layered system, using a capacitor model which is based on the schematic electrode pattern of Fig. 1. This allows us to calculate t and u_0 as a function of the applied gate voltage and the distance between the layers. Indirect excitons in CQWs are formed by two TMDC monolayers that are separated by h-BN since h-BN monolayers are characterized by a relatively small density of defects of their crystal structure monolayers. The separation between two layers of TMDC materials is calculated in steps of $D_{\mathrm{hBN}} = 0.333$ nm, corresponding to the thickness of one h-BN monolayer [47]. Using the values of the periodic potential and the interlayer distance D, we obtain from the capacitor model the values of t of the electron-hole dispersion in Eq. (2) as

$$t = \frac{1}{2}\frac{\varepsilon\varepsilon_0 A}{D}V^2,$$

where V is the potential difference applied to the electrodes, A is the area of the electrodes, and ε (ε_0) is the relative (vacuum) dielectric constant. The corresponding interaction parameter u_0 for the square electrodes with $a = 5$ nm and applied voltage $V = 20$ mV for the square lattice period $b = 20$ μm along with values of t are given in Table I. It is interesting to note that the coupling strength u_0 and the critical temperature decrease with the number of layers.

TABLE I. Results for physical parameters t, δ_0, and u_0 at the critical temperature. The latter is obtained from the calculation in Sec. III, where a phase transition occurs when $\beta t = 0.22$ and $\delta_0/t = 0.35$.

					u_0 (eV)		
N_L	D (Å)	t (meV)	T (K)	δ_0 (meV)	$\beta u_0 = -60$	$\beta u_0 = -50$	$\beta u_0 = -40$
2	6.66	2.03	107	0.71	0.553	0.461	0.369
3	9.99	1.35	71	0.47	0.369	0.307	0.246
4	13.32	1.02	54	0.36	0.277	0.231	0.184
5	16.65	0.81	43	0.28	0.221	0.184	0.148
6	19.98	0.68	36	0.24	0.184	0.154	0.123
7	23.31	0.56	31	0.20	0.158	0.132	0.105

[1] Yu. E. Lozovik and V. I. Yudson, Sov. Phys. JETP Lett. **22**, 26 (1975); Sov. Phys. JETP **44**, 389 (1976).
[2] S. I. Shevchenko, Phys. Rev. Lett. **72**, 3242 (1994).
[3] X. Zhu, P. B. Littlewood, M. S. Hybertsen, and T. M. Rice, Phys. Rev. Lett. **74**, 1633 (1995).
[4] S. Conti, G. Vignale, and A. H. MacDonald, Phys. Rev. B **57**, R6846 (1998).
[5] M. A. Olivares-Robles and S. E. Ulloa, Phys. Rev. B **64**, 115302 (2001).
[6] D. S. L. Abergel, M. Rodriguez-Vega, E. Rossi, and S. Das Sarma, Phys. Rev. B **88**, 235402 (2013).
[7] M. Zarenia, A. Perali, D. Neilson, and F. M. Peeters, Sci. Rep. **4**, 7319 (2014).
[8] M. Combescot, R. Combescot, and F. Dubin, Rep. Prog. Phys. **80**, 066501 (2017).
[9] D. V. Fil and S. I. Shevchenko, Low Temp. Phys. **44**, 867 (2018).
[10] Yu. E. Lozovik, Phys. Usp. **188**, 1203 (2018).
[11] A. Perali, D. Neilson, and A. R. Hamilton, Phys. Rev. Lett. **110**, 146803 (2013).
[12] T. Fukuzawa, E. E. Mendez, and J. M. Hong, Phys. Rev. Lett. **64**, 3066 (1990); J. A. Kash, M. Zachau, E. E. Mendez, J. M. Hong, and T. Fukuzawa, *ibid.* **66**, 2247 (1991).
[13] U. Sivan, P. M. Solomon, and H. Shtrikman, Phys. Rev. Lett. **68**, 1196 (1992).
[14] S. A. Moskalenko and D. W. Snoke, *Bose-Einstein Condensation of Excitons and Biexcitons and Coherent Nonlinear Optics with Excitons* (Cambridge University Press, New York, 2000).
[15] L. V. Butov, A. Zrenner, G. Abstreiter, G. Bohm, and G. Weimann, Phys. Rev. Lett. **73**, 304 (1994); L. V. Butov, C. W. Lai, A. L. Ivanov, A. C. Gossard, and D. S. Chemla, Nature (London) **417**, 47 (2002); L. V. Butov, A. C. Gossard, and D. S. Chemla, *ibid.* **418**, 751 (2002).
[16] L. V. Butov, J. Phys.: Condens. Matter **16**, R1577 (2004).
[17] A. V. Larionov and V. B. Timofeev, JETP Lett. **73**, 301 (2001); A. V. Gorbunov and V. B. Timofeev, *ibid.* **84**, 329 (2006).
[18] V. V. Krivolapchuk, E. S. Moskalenko, and A. L. Zhmodikov, Phys. Rev. B **64**, 045313 (2001).
[19] D. Snoke, S. Denev, Y. Liu, L. Pfeiffer, and K. West, Nature (London) **418**, 754 (2002).
[20] D. Snoke, Science **298**, 1368 (2002).
[21] R. Anankine, M. Beian, S. Dang, M. Alloing, E. Cambril, K. Merghem, C. G. Carbonell, A. Lemaitre, and F. Dubin, Phys. Rev. Lett. **118**, 127402 (2017).
[22] J. I. A. Li, T. Taniguchi, K. Watanabe, J. Hone, and C. R. Dean, Nat. Phys. **13**, 751 (2017).
[23] G. W. Burg, N. Prasad, K. Kim, T. Taniguchi, K. Watanabe, A. H. MacDonald, L. F. Register, and E. Tutuc, Phys. Rev. Lett. **120**, 177702 (2018).
[24] Yu. E. Lozovik and O. L. Berman, JETP Lett. **64**, 573 (1996).
[25] O. L. Berman, Yu. E. Lozovik, D. W. Snoke, and R. D. Coalson, Phys. Rev. B **70**, 235310 (2004).
[26] Yu. E. Lozovik and O. L. Berman, Phys. Scr. **58**, 86 (1998).
[27] G. E. Astrakharchik, J. Boronat, I. L. Kurbakov, and Yu. E. Lozovik, Phys. Rev. Lett. **98**, 060405 (2007).
[28] A. E. Golomedov, G. E. Astrakharchik, and Yu. E. Lozovik, Phys. Rev. A **84**, 033615 (2011).
[29] Y. N. Joglekar, A. V. Balatsky, and S. Das Sarma, Phys. Rev. B **74**, 233302 (2006).
[30] D. W. Snoke, in *Quantum Gases: Finite Temperature and Non-equilibrium Dynamics*, edited by N. P. Proukakis, S. A. Gardiner, M. J. Davis, and M. H. Szymanska, Cold Atom Series Vol. 1 (Imperial College Press, London, 2013), p. 419.
[31] K. Das Gupta, A. F. Croxall, J. Waldie, C. A. Nicoll, H. E. Beere, I. Farrer, D. A. Ritchie, and M. Pepper, Adv. Condens. Matter Phys. **2011**, 727958 (2011).
[32] L. V. Butov, J. Phys.: Condens. Matter **19**, 295202 (2007).
[33] V. V. Solov'ev, I. V. Kukushkin, J. Smet, K. von Klitzing, and W. Dietsche, JETP Lett. **83**, 553 (2006).
[34] M. Alloing, M. Beian, M. Lewenstein, D. Fuster, Y. González, L. González, R. Combescot, M. Combescot, and F. Dubin, Europhys. Lett. **107**, 10012 (2014).
[35] K. Cohen, Y. Shilo, K. West, L. Pfeiffer, and R. Rapaport, Nano Lett. **16**, 3726 (2016).
[36] M. Remeika, J. C. Graves, A. T. Hammack, A. D. Meyertholen, M. M. Fogler, L. V. Butov, M. Hanson, and A. C. Gossard, Phys. Rev. Lett. **102**, 186803 (2009).
[37] O. L. Berman, Yu. E. Lozovik, and G. Gumbs, Phys. Rev. B **77**, 155433 (2008).
[38] Yu. E. Lozovik and A. A. Sokolik, JETP Lett. **87**, 55 (2008); Phys. Lett. A **374**, 326 (2009).
[39] R. Bistritzer and A. H. MacDonald, Phys. Rev. Lett. **101**, 256406 (2008).
[40] O. L. Berman, R. Ya. Kezerashvili, and K. Ziegler, Phys. Rev. B **85**, 035418 (2012).
[41] D. K. Efimkin, Yu. E. Lozovik, and A. A. Sokolik, Phys. Rev. B **86**, 115436 (2012).
[42] J. P. Eisenstein and A. H. MacDonald, Nature (London) **432**, 691 (2004).
[43] A. Kormányos, G. Burkard, M. Gmitra, J. Fabian, V. Zólyomi, N. D. Drummond, and V. Fal'ko, 2D Mater. **2**, 022001 (2015).

[44] K. F. Mak, C. Lee, J. Hone, J. Shan, and T. F. Heinz, Phys. Rev. Lett. **105**, 136805 (2010).
[45] D. Xiao, G. B. Liu, W. Feng, X. Xu, and W. Yao, Phys. Rev. Lett. **108**, 196802 (2012).
[46] K. F. Mak, K. He, C. Lee, G. H. Lee, J. Hone, T. F. Heinz, and J. Shan, Nat. Mater. **12**, 207 (2013).
[47] M. M. Fogler, L. V. Butov, and K. S. Novoselov, Nat. Commun. **5**, 4555 (2014).
[48] E. V. Calman, C. J. Dorow, M. M. Fogler, L. V. Butov, S. Hu, A. Mishchenko, and A. K. Geim, Appl. Phys. Lett. **108**, 101901 (2016).
[49] F.-C. Wu, F. Xue, and A. H. MacDonald, Phys. Rev. B **92**, 165121 (2015).
[50] O. L. Berman and R. Ya. Kezerashvili, Phys. Rev. B **93**, 245410 (2016).
[51] O. L. Berman and R. Ya. Kezerashvili, Phys. Rev. B **96**, 094502 (2017).
[52] N. Dupuis, Phys. Rev. B **70**, 134502 (2004).
[53] J. M. Ziman, *Principles of the Theory of Solids*, 2nd ed. (Cambridge University Press, Cambridge, 1979).
[54] S. H. Simon, *The Oxford Solid State Basics* (Oxford University Press, Oxford, 2013).
[55] N. W. Ashcroft and N. D. Mermin, *Solid State Physics* (Saunders College, New York, 1976).
[56] J. R. Schrieffer, *Theory of Superconductivity* (Benjamin, New York, 1964).
[57] P. G. de Gennes, *Superconductivity of Metals and Alloys* (Benjamin, New York, 1966).
[58] O. L. Berman, R. Ya. Kezerashvili, and K. Ziegler, Phys. E (Amsterdam, Neth.) **71**, 7 (2015).
[59] Yu. E. Lozovik, S. P. Merkulova and A. A. Sokolik, Phys. Usp. **178**, 757 (2008).
[60] H. Min, R. Bistritzer, J.-J. Su, and A. H. MacDonald, Phys. Rev. B **78**, 121401(R) (2008).
[61] M. Yu. Kharitonov and K. B. Efetov, Phys. Rev. B **78**, 241401(R) (2008).
[62] Yu. E. Lozovik and A. A. Sokolik, Eur. Phys. J. B **73**, 195 (2010).
[63] Yu. E. Lozovik, S. L. Ogarkov, and A. A. Sokolik, Phys. Rev. B **86**, 045429 (2012).
[64] T. Stroucken, J. H. Gronqvist, and S. W. Koch, Phys. Rev. B **87**, 245428 (2013).
[65] J.-J. Su and A. H. MacDonald, Phys. Rev. B **95**, 045416 (2017).
[66] P. Cudazzo, I. V. Tokatly, and A. Rubio, Phys. Rev. B **84**, 085406 (2011).
[67] N. S. Rytova, Moscow Univ. Phys. Bull. **22**, 18 (1967).
[68] L. V. Keldysh, Pis'ma Zh. Eksp. Teor. Fiz. **29**, 716 (1979) [JETP Lett. **29**, 658 (1979)].
[69] R. Ya. Kezerashvili, Few-Body Syst. **60**, 52 (2019).
[70] L. D. Landau and E. M. Lifshitz, *Statistical Physics*, Part 1, 3rd ed. (Pergamon, Oxford, 1980).
[71] E. M. Lifshitz and L. P. Pitaevskii, *Statistical Physics*, Part 2 (Pergamon, Oxford, 1980).
[72] H. Lee, K. Paeng, and I. S. Kim, Synth. Met. **244**, 36 (2018).
[73] E. Suárez Morell, J. D. Correa, P. Vargas, M. Pacheco, and Z. Barticevic, Phys. Rev. B **82**, 121407(R) (2010).
[74] R. Bistritzer and A. H. MacDonald, Proc. Natl. Acad. Sci. USA **108**, 12233 (2011).
[75] G. Li, A. Luican, J. M. B. Lopes dos Santos, A. H. Castro Neto, A. Reina, J. Kong, and E. Y. Andrei, Nat. Phys. **6**, 109 (2010).
[76] G. L. Yu, R. V. Gorbachev, J. S. Tu, A. V. Kretinin, Y. Cao, R. Jalil, F. Withers, L. A. Ponomarenko, B. A. Piot, M. Potemski, D. C. Elias, X. Chen, K. Watanabe, T. Taniguchi, I. V. Grigorieva, K. S. Novoselov, V. I. Fal'ko, A. K. Geim, and A. Mishchenko, Nat. Phys. **10**, 525 (2014).
[77] X. Lin and D. Tománek, Phys. Rev. B **98**, 081410(R) (2018).
[78] X. Lin, D. Liu, and D. Tománek, Phys. Rev. B **98**, 195432 (2018).
[79] K. Ziegler and A. Sinner, Europhys. Lett. **119**, 27001 (2017).
[80] A. Gonis, *Green Functions for Ordered and Disordered Systems* (North-Holland, Amsterdam, 1992).
[81] A. Bianconi, A. Valletta, A. Perali, and N. L. Saini, Solid State Commun. **102**, 369 (1997).
[82] A. Bianconi, A. Valletta, A. Perali, and N. L. Saini, Phys. C (Amsterdam, Neth.) **296**, 269 (1998).
[83] M. Zarenia, A. Perali, F. M. Peeters, and D. Neilson, Sci. Rep. **6**, 24860 (2016).
[84] K. Tran, G. Moody, F. Wu, X. Lu, J. Choi, K. Kim, A. Rai, D. A. Sanchez, J. Quan, A. Singh, J. Embley, A. Zepeda, M. Campbell, T. Autry, T. Taniguchi, K. Watanabe, N. Lu, S. K. Banerjee, K. L. Silverman, S. Kim, E. Tutuc, L. Yang, A. H. MacDonald, and X. Li, Nature (London) **567**, 71 (2019).
[85] A. F. Andreev and I. M. Lifshitz, Sov. Phys. JETP **29**, 1107 (1969).
[86] G. V. Chester, Phys. Rev. A **2**, 256 (1970).
[87] M. Boninsegni, A. B. Kuklov, L. Pollet, N. V. Prokof'ev, B. V. Svistunov, and M. Troyer, Phys. Rev. Lett. **97**, 080401 (2006).
[88] A. A. Abrikosov, L. P. Gorkov, and I. E. Dzyaloshinski, *Methods of Quantum Field Theory in Statistical Physics* (Dover, New York, 1975).
[89] D. Y. Qiu, F. H. da Jornada, and S. G. Louie, Phys. Rev. Lett. **111**, 216805 (2013).
[90] O. L. Berman, R. Ya. Kezerashvili, Yu. E. Lozovik, and K. Ziegler, Phys. E (Amsterdam, Neth.) **92**, 1 (2017).